DOI: 10.1002/cphc.201200314

The Chemical Bond in Carbonyl and Sulfinyl Groups Studied by Soft X-ray Spectroscopy and ab Initio Calculations

Kaan Atak,[a] Nicholas Engel,[a] Kathrin M. Lange,[a] Ronny Golnak,[a] Malte Gotz,[a] Mikhail Soldatov,[a, e] Jan-Erik Rubensson,[c] Nobuhiro Kosugi,[d] and Emad F. Aziz*[a, b]

The acetone and dimethyl sulfoxide (DMSO) molecules have been thoroughly studied over the years.[1] Although their physical properties are very different, they are both widely used as solvents for various chemicals. In addition, DMSO plays an important role in atmospheric chemistry as it is considered an intermediate in the atmospheric oxidation of dimethyl sulfide,[2] and it has important pharmaceutical and biological applications. The electronic structure and dynamics of acetone have recently been investigated with vacuum ultraviolet absorption spectroscopy[3] and resonant inelastic X-ray scattering (RIXS),[4] demonstrating that intermolecular interactions in the liquid phase do not affect the intra-molecular interactions appreciably. Studies using Monte Carlo simulations revealed that the dominant intermolecular interaction is steric rather than electrostatic in liquid acetone.[5] DMSO has been given relatively less attention experimentally, in spite of its importance and intriguing properties. Compared to acetone and other aprotic solvents, it has a very large dipole moment and high boiling and melting points (Table 1). The differences can primarily be explained by the large polarity of the sulfinyl group in DMSO compared to the carbonyl group in acetone, but the detailed mechanisms behind the phenomenology are still under debate. In ab initio molecular orbital calculations Pietro et al. found that the sulfinyl group becomes zwitterionic ($S^+ \rightarrow O^-$) or forms a double bond (S=O), depending on the basis set[11] (inset of Figure 1 a). Although the double-bond picture seems to be widely accepted Clark et al[6] recently showed on a theoretical basis that the sulfur-oxygen linkage must be regarded as a coordinate covalent (single) bond.

Table 1. Experimental physical properties of DMSO and acetone.[6,10]

Compound	Dielectric constant	Dipole moment [D]	Melting point [°C]	Boiling point [°C]
DMSO	47.24	3.96	17.89	189
Acetone	21.01	2.88	−94.7	56.05

[a] Dr. K. Atak, N. Engel, K. M. Lange, R. Golnak, M. Gotz, M. Soldatov, Prof. Dr. E. F. Aziz
Functional Materials in Solution
Helmholtz-Zentrum Berlin für Materialien und Energie
Albert-Einstein-Str. 15, 12489 Berlin (Germany)
Fax: (+49) 30 806214757
E-mail: emad.aziz@helmholtz-berlin.de

[b] Prof. Dr. E. F. Aziz
Freie Universität Berlin, FB Physik
Arnimallee 14, 14159 Berlin (Germany)

[c] Prof. Dr. J.-E. Rubensson
Department of Physics and Astronomy
Uppsala University Box 516, 751 20 Uppsala (Sweden)

[d] Prof. Dr. N. Kosugi
Institute for Molecular Science, Myodaiji
Okazaki 444-8585 (Japan)

[e] M. Soldatov
Research Center for Nanoscale Structure of Matter
Southern Federal University, Sorge 5
Rostov-na-Donu 344090 (Russia)

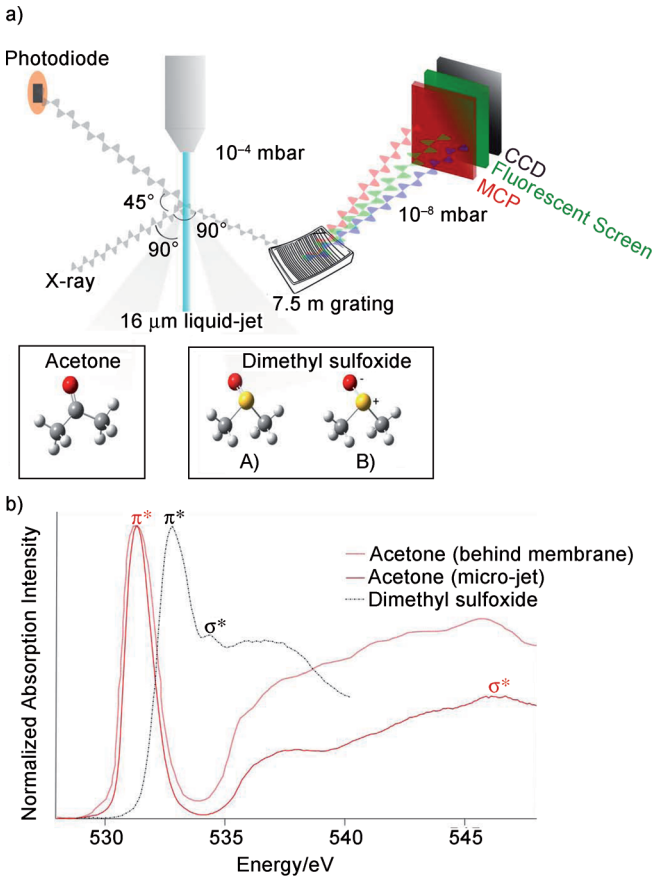

Figure 1. a) Schematic presentation for the LiXEdrom setup. b) The total fluorescence yield obtained from acetone and DMSO respectively (with a comparison spectrum from literature).

In this picture, the large dipole moments and dielectric constants as well as the high boiling points and solvent power of DMSO can be understood. On the other hand, it does not explain why the molecule is relatively inert. In addition, molecular dynamics simulations have suggested that the partial charges in the liquid DMSO might be different from those of an isolated molecule.[7]

Herein, we use X-ray absorption (XA), emission (XE), and resonant inelastic X-ray scattering (RIXS) at the oxygen K-edge to study the carbonyl and sulfinyl groups of acetone and DMSO

in liquid form. Our recently developed high-resolution X-ray emission spectrometer that was specifically designed for measurements with a liquid micro-jet is used for this study.[8] A schematic presentation for the setup is shown in Figure 1a. The XE spectra have been assigned with the help of ab initio Hartree–Fock and configuration interaction (CI) calculations using the GSCF3 code.[9] We correlate the origin of the solvent power of DMSO to the partial negative and positive charge located on the oxygen and the sulfur of the sulfinyl group. The molecular orbitals of acetone and DMSO as well as the energy gap allow us to draw detailed information concerning the chemical stability of these solvents and its electrophilic and nucleophilic reactivity.

Oxygen K-edge TFY spectra of acetone and DMSO are shown in Figure 1b. A reference spectrum for acetone obtained from a flow cell separating the liquid acetone from the vacuum by Si_3N_4 membrane measured by Tokushima et al. (dashed curve) is also included.[11] The XA spectrum of acetone is dominated by the transition from the oxygen 1 s orbital to the lowest unoccupied molecular orbital (LUMO) at 531.3 eV. The LUMO has π^* character and due to the attractive potential of the core hole, the O 1 $s^{-1}\pi^*$ resonance appears below the ionization limit.[12] The spectral features are much broader than the gas-phase spectrum[13] and it is not trivial to determine the exact position and the origin of the features at higher energy. Nevertheless, from the interpretation of the gas-phase features by Hitchcock et al.[13] we can attribute the broad peak between 535 and 538 eV to unoccupied valence states of oxygen *p*-character. In the gas-phase case we would expect to find Rydberg states in the region between 541 and 544 eV[1h,k,14] followed by doubly excited states at higher energies. Rydberg states could be mixed with carbon-derived anti-bonding orbitals of the same symmetry, and in the liquid further smearing of the spectral features is due to the interaction with neighboring molecules. Finally, we assign the absorption peak centered at 547 eV to the shape resonance (σ^*), in analogy with the gas-phase assignment.[15]

The peak at the lowest energy in the DMSO spectrum is found at 532.8 eV. Following Sze et al., we assign this peak to a transition from the oxygen 1 s orbital to the LUMO, which, also in DMSO primarily has π^* character.[16] Indeed, the π^* resonance is only observed for molecules which have π bonding.[17] Thus, already this observation suggests the sulfinyl group rather has a double (S=O) bond than a single ($S^+ \rightarrow O^-$) bond.[6] The features at higher energy of DMSO are most likely due to transitions to MOs with local oxygen *p*-character. The peak at 534.2 eV is of low-lying σ^* character in the relatively weak sulfur-oxygen bond. For molecules with a carbonyl group, the σ^* resonance lies in the continuum above the ionization potential (IP) due to its relatively strong anti-bonding character. Note that the oxygen 1 s IP of DMSO in gas phase is at 536.67 eV as obtained from X-ray photoelectron spectroscopy.[18]

The RIXS spectra of acetone excited on the oxygen 1 $s^{-1}\pi^*$ resonance and the high-energy non-resonantly excited XE spectra are presented in Figure 2. The spectra are due to the radiative decay of core-excited states as an electron from the

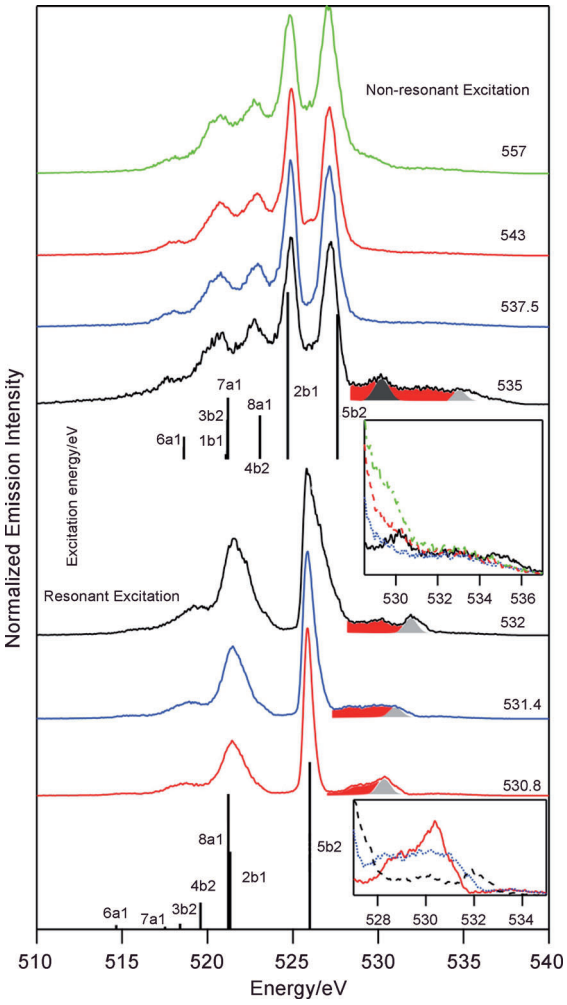

Figure 2. RIXS and XE spectra for acetone together with the calculated spectra (the insets are not intensity-normalized).

valence orbitals fills the core hole. In the RIXS process, also the excited electron can fill the core in transitions to the electronic ground state, giving rise to a quasi-elastic line with only vibrational energy losses. The highest energy feature in Figure 2, marked with a Gaussian fit (shaded gray), corresponds to the elastic scattering and is used for energy calibration. Apart from this feature, there are unresolved vibrational progressions.[4] The dominant contribution is due to the C–O stretching mode (shaded red). In order to understand the origin of the rest of the emission peaks, we use the MO picture. According to Zheng et al.,[19] the occupied orbitals for a single acetone molecule with the C_{2v} symmetry in the increasing energy order are: $1a_1$, $2a_1$, $1b_2$, $3a_1$, $4a_1$, $5a_1$, $2b_2$, $6a_1$, $3b_2$, $7a_1$, $1b_1$, $1a_2$, $8a_1$, $4b_2$, $2b_1$, and $5b_2$ (HOMO). In Figure 2, the calculated XE peaks are shown as bars below the experimental results. Accordingly, relaxation from the valence $5b_2$, $4b_2$, $3b_2$, $2b_1$, $1b_1$, $8a_1$, $7a_1$, $6a_1$ orbitals (emission from a_2 type orbitals is dipole forbidden) to the core-hole $1a_1$ takes place for both non-resonant and resonant cases. The spectral features of the non-resonant series are in good agreement with the theoretical predictions. A feature unaccounted for by the calculation appears at emission ener-

gies above the $5b_2$ (HOMO) peak at 535 eV excitation energy in a long tail and peak at 530 eV (shaded black). Here we are exciting the $1a_1$ electron to mixed valence-Rydberg states, requiring energy of 535 eV according to the XA spectrum (see Figure 1 b). We assign the long tail to unresolved vibrational progressions associated with the electronic ground state as the excited electron refills the core hole. The peak at 530 eV emission energy could be due to mixing with the 1 $s^{-1}\pi^*$ state. At higher excitation energies, a high-energy shoulder on the HOMO peak appears (Figure 2 upper inset). The energy position of the peak is close to the $3b_1$ LUMO peak, and consequently it is tempting to assign it to emission from the $3b_1$ LUMO orbital populated in a shake-up process, or via screening from the surrounding molecules. Alternatively, this intensity can be satellites due to multiply ionized states populated via shake-off in the excitation step. The appearance of such satellites complies with the expectations for a free molecule and shows that the extra vacancies are not screened in the liquid during the core-hole lifetime (<4 fs).[20]

The RIXS and XE spectra of DMSO (Figure 3) show quite different trends compared to the acetone case. At the first resonant excitation, the elastic scattering peaks are less prominent than in acetone. This directly demonstrates that the excited electron is less localized than the electron in the 1 $s^{-1}\pi^*$ excitation in acetone. Another distinction from the acetone case is the shift of the valence peaks towards higher energies as the excitation energy increases within the first resonance. For higher energy excitation, beyond the first resonance, the valence peaks do not show any shift energetically or any change in the relative structure. DMSO has a lower symmetry (C_s symmetry)[21] compared to acetone. The molecule has only one symmetry element, a mirror plane bisecting the molecule between the two methyl groups. According to the theoretical analysis of the MOs, the occupied orbitals for a single molecule are: 1a′, 2a′, 1a″, 3a′, 4a′, 5a′, 2a″, 6a′, 7a′, 8a′, 3a″, 9a′, 10a′, 4a″, 11a′, 5a″, 12a′, 6a″, 13a′, 7a″, and 14a′ as the HOMO. 15a′ and 8a″ are the close-lying LUMO and LUMO+1, respectively. In Figure 3, the calculated peaks are shown along with the experimental results. Hereby, another interesting distinction from the acetone case arises. At the first resonance, both, 15a′ and to 8a″ excitations, theoretically at 532.8 and 533.2 eV, respectively, may contribute. Their intensities are predicted to be different, the 8a″ excitation being less probable by a factor of 0.36. Based on the calculations of the RIXS spectra we can attribute the main variation in the resonantly excited spectra to a superposition of scattering involving the 15a′ and 8a″ channels (Figure 3). At 532.3 eV excitation energy the 15a′ channel is dominant. By increasing the excitation energy, the 8a″ channel is progressively mixed in. Another remarkable difference from the acetone case in the series of XE spectra excited at higher energy is the apparent absence of high-energy satellites. This can be understood in both interpretation schemes that we considered plausible in the acetone case. Any screening from the surrounding molecules to the LUMO or LUMO+1 orbitals would be much weaker in DMSO as these orbitals are much less localized compared to acetone. Any additional valence ionization due to shake-off would also have less effect

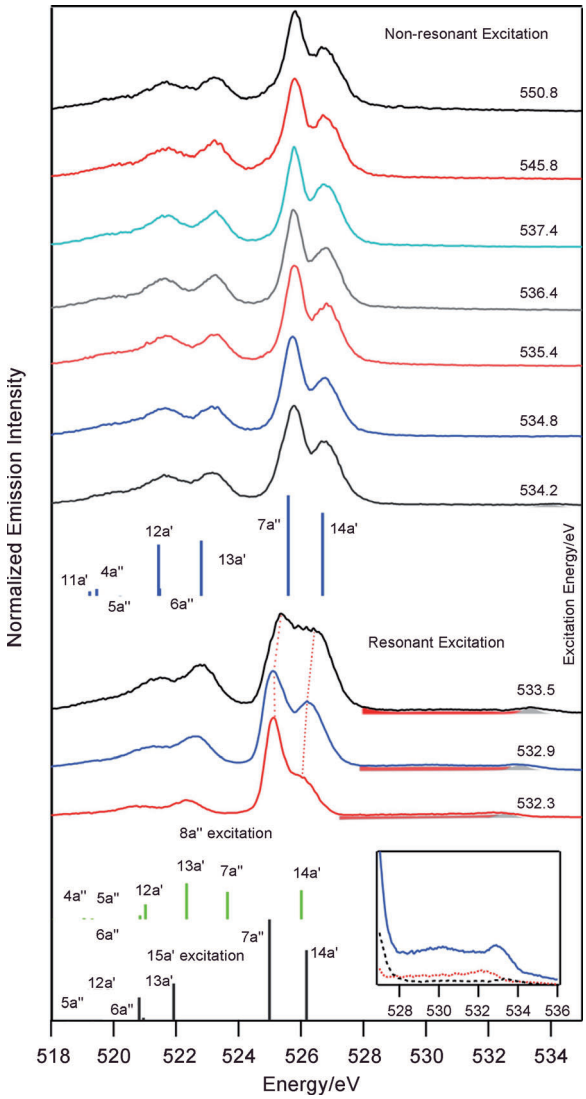

Figure 3. RIXS and XES spectra obtained from dimethyl sulfoxide together with the calculated spectra (the inset is not intensity-normalized).

in DMSO as also the valence orbitals are more diffuse than in acetone.

Finally, we highlight the striking similarity between the acetone and DMSO XE spectra in Figure 4. By stretching the energy scale of the DMSO spectrum, we get a very good concordance between the spectra. This may be surprising considering the large difference between the molecules. As the spectra reflect the local electronic structure at the oxygen site, this result suggests that the oxygen atom interacts in a similar way with neighboring atoms in DMSO and acetone. The spacing between the peaks is directly related to the spacing between the final states. In the MO picture, the wider spacing between the valence orbitals in acetone is interpreted as due to a larger overlap between the atomic orbitals than the corresponding overlap in DMSO. The difference in overlap in the bonding molecular orbitals can be directly associated with the difference in strength of the C–O and S–O bonds of the two molecules. Besides the energy spacing, the largest difference between the

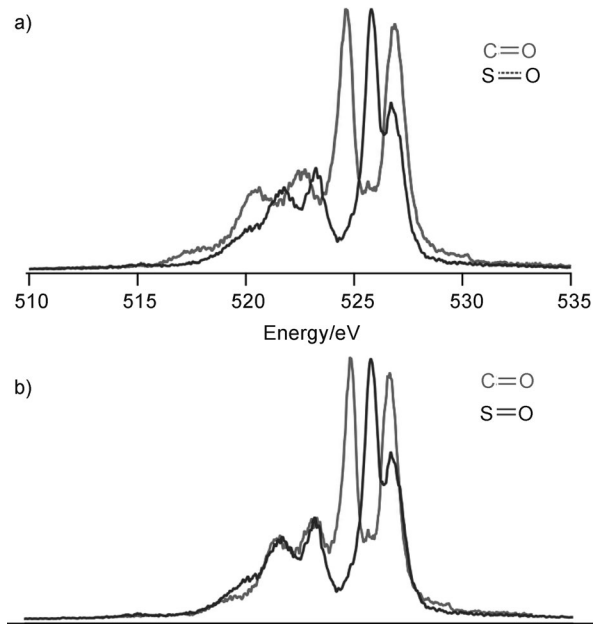

Figure 4. a) Comparison of the XE spectra of acetone and DMSO as obtained experimentally in the non-resonant regime. b) Stretching of the XE spectrum of DMSO to fit that of acetone. The comparison demonstrates that the local electronic structure at the oxygen atom is similar in the C=O and S=O bonds, albeit with a weaker interaction in the latter case.

two spectra concerns the two peaks at the highest energy. In both spectra, the highest-energy peak can be assigned to final states with a vacancy in the HOMOs. The difference between the two spectra is that the intensity in the DMSO spectrum is about half the corresponding intensity in the acetone spectrum. Assuming the validity of the one-center intensity model this indicates that the HOMO in DMSO has less oxygen *p*-character compared to the acetone HOMO. In both molecules these orbitals are often termed oxygen "lone-pair" orbitals, and the present results indicate that the lone-pair character of the HOMO is much less pronounced in DMSO. The second peak corresponding to final states with a vacancy in HOMO-1 shows a strong additional energy shift in Figure 4 when comparing acetone and DMSO spectra. In acetone, the HOMO-1 orbital is π-bonding, with coinciding nodal and molecular planes. In DMSO the HOMO-1 orbital has also π-bonding character but the situation is complicated in the molecular geometry where the S–O bond is bent out of the molecular plane, and the antibonding interaction with the methyl groups is more prominent than for acetone. The π-bonding due to the HOMO-1 in acetone is thus much weaker in DMSO, reflected in the additional energy difference between the corresponding peaks.

It is well known that DMSO has a large dipole moment[10a] with excess negative charge at the oxygen site. One may have expected that this would resulted in an increased oxygen weight of molecular orbitals associated with large polarizability, reflected in spectral intensity redistribution. The small differences between the spectra of acetone and DMSO show that the oxygen *p*-character of the orbitals is affected in a largely homogenous way. Comparing acetone and DMSO, there is, however, a small redistribution of intensity from the "lone pair" peak to the low-energy part of the spectra, which according to our calculations corresponds to the $6a_1$ orbital in acetone (see Figure 2). This intra-molecularly delocalized orbital has σ-antibonding character with respect to the C–O bond. The increasing relative XE intensity in the sulfinyl group associated with this feature suggests that this orbital is particularly polarized towards the oxygen atom, thus weakening the S–O bond further. Accordingly, we could conclude from this picture that the partially charged oxygen in the sulfinyl group originated from the deeper valence orbitals than the highest ones. This would give a higher dipole moment for the DMSO compared to acetone. According to the frontier molecular orbital theory of chemical reactivity, the formation of a transition state is due to an interaction between the frontier orbitals (HOMO and LUMO) of reacting species.[22] Thus, as the partial charge comes from deeper valence orbitals, it will interact with the neighboring molecules purely electrostatically. In other words, if the partial charges come from the HOMO, we would expect a stronger interaction between DMSO molecules and any solute.

Figure 5 presents a conclusive picture for the valence and the unoccupied MOs of both acetone and DMSO. In both spectra the core-hole effects are assumed to be similar enabling us for a direct comparison. In the bottom of the Figure, we draw

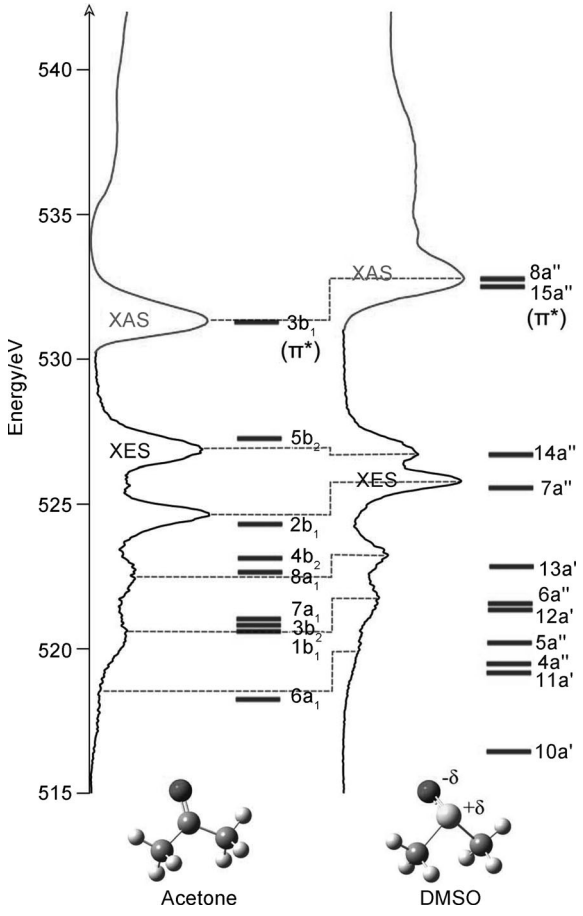

Figure 5. The MOs of acetone and DMSO, as obtained from the XA and XE spectra, are combined with the theoretical simulation. Bottom: schematic representation of the carbonyl and sulfinyl groups of acetone and DMSO based on our experimental observations.

a schematic picture for both acetone and DMSO structure according to the obtained MOs information from the valence and the un-occupied states. A clear distinguishable difference between the acetone and the DMSO is the HOMO–LUMO energy gap. Where in acetone it is 4.2 eV, in DMSO it is 6 eV. It is quite interesting to observe that the ratio of the dipole moments for DMSO and acetone is 1.4, which is equal to the energy gap ratio.

The HOMO–LUMO gap is an important stability index for the molecules.[23] A large HOMO–LUMO gap implies high stability, which reflects low reactivity toward chemical reactions.[22] This is in a supportive agreement with our previous conclusion that the DMSO solvent power is based on electrostatic interaction. Indeed, according to Pearson, the increase of the HOMO–LUMO gap would reveal on the hardness of the molecule.[24] Hardness is closely related to the polarizability, since a decrease of the energy gap usually leads to easier polarization of the molecule.[24] The majority of chemical reactions take place at the position and in the orientation where overlap of the HOMO and LUMO of the respective reactants can reach a maximum.[22] For donor molecule, the HOMO density is critical to the charge transfer (electrophilic electron density) and in the case of an acceptor molecule the LUMO density is important (nucleophilic electron density). This also proposes that DMSO is more nucleophilic and electrophilic than acetone, since it can give and receive electron density easier.

The investigation of the local electronic structure of acetone and DMSO adds significantly on the power of X-ray absorption and emission on the micro-jet using the soft X-ray photons. The high-energy resolution of our recent spectrometer ($<$ 200 meV at the oxygen K-edge) and the ability of the method to probe ultrafast dynamics (core–hole lifetime of <4 fs[20]) allows us to address the structure of the carbonyl and the sulfinyl chemical bonds in solution. The obtained electronic information show that while the carbonyl group has a stronger and shorter double bond, the sulfinyl has a longer double bond. The partial charges on the oxygen and the sulfur rather originate from deeper valence orbitals than the highest occupied ones. This correlates the high solvent power of DMSO to pure electrostatic interaction with the neighboring molecule. The wider HOMO–LUMO gap of the DMSO as compared to acetone explains its chemical stability and its stronger nucleophilic and electrophilic properties. The present work marks a significant step forward towards understanding chemical bonds in solution.[25]

Experimental Section

The experiments were conducted using soft X-rays obtained from the U41 PGM undulator beamline of the synchrotron light facility BESSY II, at Helmholtz-Zentrum Berlin. Experimental details have been described previously.[8] Fresh samples were constantly introduced using a liquid micro jet of ~16 μm diameter. The total fluorescence yield (TFY) XA spectra were recorded with a InGaAsP diode. For the XE measurements of the oxygen emission lines a Rowland spectrometer with a grating of 7.5 m radius and a line density of 1200 lines per mm was used. The calibration of the TFY spectra was done according to Tokushima et al. based on their XA measurement of acetone.[11] The emission spectra were calibrated using the TFY spectra together with the elastic scattering peaks in the XE spectra. The estimated temperature of the liquids in the probing zone is around 15 °C.[26]

To understand the molecular orbital (MO) origin of the emission peaks, ab initio quantum chemical calculations were carried out using the GSCF3 code. The present calculations ignore effects of molecular vibrations and dynamics as well as intermolecular interactions which have been already discussed in detail for acetone.[4] Non-resonant and resonant XE spectra were calculated for the ground state geometry as transitions between core and valence ionized states and between core-π^* and valence-π^* excited states, respectively. Primitive basis functions were taken from (533/53), (73/7), and (63/5) contracted Gaussian-type functions of Huzinaga et al.[27] which are augmented with d-type polarization functions $\alpha = 1.154$ for O and 0.421 for S. The contraction Scheme was (412121/41111/1*) for S, (3111121/31111/1*) for O, (621/41) for C, and (32) for H atoms. Diffuse functions were not included in this calculation as the Rydberg states are out of the present scope. The O 1 s ionized and O 1 s-π^* excited states were calculated within ΔSCF (self-consistent field) approaches. The valence ionized states were obtained by single hole, double hole single particle, and triple hole double particle (1 h, 2 h1p and 3 h2p) configuration interactions (CI) involving single and double substitutions from all valence ionized states by using the Hartree–Fock orbitals. Valence excited states are complicated and 1 h1p components giving transition probabilities are distributed across many excited states in large scale CI, which makes it difficult to interpret moderate-resolution spectral profiles. Therefore, the valence-excited states were obtained by 1 h1p CI among all the singly excited configurations from the Hartree–Fock ground state configuration. This type of CI gives upper bound state energies for primary states of valence excitations.

Acknowledgements

This work was supported by the Helmholtz-Gemeinschaft via the VH-NG-635 grant (E.F.A.) and the European Research Council grant No. 279344 (E.F.A.). K. A. would like to acknowledge the financial support of the Vehbi Koc Foundation Istanbul as of the postdoctoral scholarship in Aziz team.

Keywords: ab initio calculations · acetone · chemical bond · dimethyl sulfoxide · X-ray spectroscopy

[1] a) P. W. Allen, H. J. M. Bowen, L. E. Sutton, O. Bastiansen, *Transactions of the Faraday Society* **1952**, *48*, 991 – 995; b) D. Cremer, J. S. Binkley, J. A. Pople, W. J. Hehre, *J. Am. Chem. Soc.* **1974**, *96*, 6900 – 6903; c) D. Cruickshank, *J. Chem. Soc.* **1961**, 5486; d) H. Hollenstein, H. H. Gunthard, *J. Mol. Spectrosc.* **1980**, *84*, 457 – 477; e) W. Moffitt, *Proc. R. Soc. London Ser. A* **1950**, *200*, 409 – 428; f) C. C. Price, S. Oae, *Sulfur Bonding*, The Roland Press Co., New York, **1960**; g) J. D. Swalen, C. C. Costain, *J. Chem. Phys.* **1959**, *31*, 1562 – 1574; h) J. P. Doering, R. Mcdiarmid, *J. Chem. Phys.* **1982**, *76*, 1838 – 1844; i) M. S. Gopinath, P. T. Narasimh, *J. Magn. Reson.* **1972**, *6*, 147; j) V. I. Khaustova, *Izv. Vyssh. Uchebn. Zaved. Fiz.* **1978**, 19 – 22; k) M. Merchán, B. O. Roos, R. McDiarmid, X. Xing, *J. Chem. Phys.* **1996**, *104*, 1791 – 1804; l) W. J. Pietro, M. M. Francl, W. J. Hehre, D. J. Defrees, J. A. Pople, J. S. Binkley, *J. Am. Chem. Soc.* **1982**, *104*, 5039 – 5048.

[2] I. Barnes, J. Hjorth, N. Mihalopoulos, *Chem. Rev.* **2006**, *106*, 940 – 975.

[3] M. Nobre, A. Fernandes, F. F. da Silva, R. Antunes, D. Almeida, V. Kokhan, S. V. Hoffmann, N. J. Mason, S. Eden, P. Limao-Vieira, *Phys. Chem. Chem. Phys.* **2008**, *10*, 550 – 560.
[4] Y. P. Sun, F. Hennies, A. Pietzsch, B. Kennedy, T. Schmitt, V. N. Strocov, J. Andersson, M. Berglund, J. E. Rubensson, K. Aidas, F. Gel'mukhanov, M. Odelius, A. Foehlisch, *Phys. Rev. B* **2011**, *84*, 132202.
[5] a) P. Jedlovszky, G. Palinkas, *Molecular Physics* **1995**, *84*, 217 – 233; b) M. Ferrario, M. Haughney, I. R. Mcdonald, M. L. Klein, *J. Chem. Phys.* **1990**, *93*, 5156 – 5166; c) M. G. Giorgini, M. Musso, H. Torii, *J. Phys. Chem. A* **2005**, *109*, 5846 – 5854.
[6] T. Clark, J. S. Murray, P. Lane, P. Politzer, *J. Mol. Model.* **2008**, *14*, 689 – 697.
[7] A. Vishnyakov, A. P. Lyubartsev, A. Laaksonen, *J. Phys. Chem. A* **2001**, *105*, 1702 – 1710.
[8] a) K. M. Lange, R. Konnecke, S. Ghadimi, R. Golnak, M. A. Soldatov, K. F. Hodeck, A. Soldatov, E. F. Aziz, *Chem. Phys.* **2010**, *377*, 1 – 5; b) K. M. Lange, R. Konnecke, M. Soldatov, R. Golnak, J. E. Rubensson, A. Soldatov, E. F. Aziz, *Angew. Chem.* **2011**, *123*, 10809 – 10813; *Angew. Chem. Int. Ed.* **2011**, *50*, 10621 – 10625.
[9] N. Kosugi, H. Kuroda, *Chem. Phys. Lett.* **1980**, *74*, 490 – 493.
[10] a) H. Dreizler, G. Dendl, *Z. Naturforsch.* **1964**, *A19*, 512; b) D. R. Lide, *Handbook of Chemistry and Physics, 87th ed.*, CRC, Boca Raton, FL, **2006**.
[11] T. Tokushima, Y. Horikawa, Y. Harada, O. Takahashi, A. Hiraya, S. Shin, *Phys. Chem. Chem. Phys.* **2009**, *11*, 1679 – 1682.
[12] Y. Jugnet, F. J. Himpsel, P. Avouris, E. E. Koch, *Phys. Rev. Lett.* **1984**, *53*, 198 – 201.
[13] A. P. Hitchcock, C. E. Brion, *J. Electron Spectrosc. Relat. Phenom.* **1980**, *19*, 231 – 250.
[14] R. Mcdiarmid, *J. Chem. Phys.* **1991**, *95*, 1530 – 1536.
[15] J. L. Dehmer, D. Dill, *Phys. Rev. Lett.* **1975**, *35*, 213 – 215.
[16] K. H. Sze, C. E. Brion, M. Tronc, S. Bodeur, A. P. Hitchcock, *Chem. Phys.* **1988**, *121*, 279 – 297.
[17] J. Stöhr, *NEXAFS Spectroscopy*, Springer-Verlag, Heidelberg, **1992**.
[18] W. L. Jolly, K. D. Bomben, C. J. Eyermann, *At. Data Nucl. Data Tables* **1984**, *31*, 433 – 493.
[19] Y. Zheng, J. J. Neville, C. E. Brion, Y. Wang, E. R. Davidson, *Chem. Phys.* **1994**, *188*, 109 – 129.
[20] E. F. Aziz, N. Ottosson, M. Faubel, I. V. Hertel, B. Winter, *Nature* **2008**, *455*, 89 – 91.
[21] R. Thomas, Cb. Shoemake, K. Eriks, *Acta Cryst.* **1966**, *21*, 12.
[22] K. Fukui, *Theory of Orientation and Stereoselection*, Springer, New York, **1975**.
[23] M. Karelson, V. S. Lobanov, A. R. Katritzky, *Chem. Rev.* **1996**, *96*, 1027 – 1043.
[24] R. G. Pearson, *J. Org. Chem.* **1989**, *54*, 1423 – 1430.
[25] K. M. Lange, A. Kothe, E. F. Aziz, *Phys. Chem. Chem. Phys.* **2012**, *14*, 5331 – 5338.
[26] K. M. Lange, M. Soldatov, R. Golnak, M. Gotz, N. Engel, R. Könnecke, J.-E. Rubensson, E. F. Aziz, *Phys. Rev. B* **2012**, *85*, 155104.
[27] S. Huzinaga, M. Klobukowski, Y. Sakai, *J. Phys. Chem.* **1984**, *88*, 4880 – 4886.

Received: April 10, 2012
Published online on June 21, 2012

